

The Fault Diagnosis of the Rolling Bearing Based on the LMD and Time-frequency Analysis

Jun Ma¹, Jiande Wu*,^{1,2} and Xuyi Yuan¹

¹Faculty of Information Engineering and Automation,
Kunming University of Science and Technology, Kunming 650500, China

²Engineering Research Center for Mineral Pipeline Transportation YN,
Kunming 650500, China

majun_km@foxmail.com

Abstract

The rolling bearing vibration is a complex, non-stationary and dynamic process. The vibration signal can not be described through a fixed time or frequency function. This increases the difficulty of fault diagnosis. Therefore, this paper proposed a rolling bearing fault diagnosis method based on local mean decomposition (LMD) and time-frequency analysis. Firstly, we need to draw time-domain waveform and power spectrum of vibration signal in this method. Secondly, we can gain the energy density distribution of signal using directly time-frequency analysis of signal, the time-frequency analysis of intrinsic mode function (IMF) and the time-frequency analysis of production function (PF). We gain the IMF by decomposing the original signal by the ensemble empirical mode decomposition (EEMD), and after the original signal is decomposed by the local mean decomposition, we gain the PF. Finally, according to the energy density distribution of signal, diagnose the fault of the rolling bearing. The simulation results show that we can gain the clearer the energy density distribution using the time-frequency of PF of signal to diagnose fault and improve the reliability of the fault diagnosis

Keywords: Rolling Bearing; EEMD; LMD; time-frequency analysis; fault diagnosis

1. Introduction

The rolling bearing is one of the most important and easily damaged parts of the rotating machinery. The bearing faults may generate seriously equipment damage and even cause catastrophic accidents. Therefore, the fault diagnosis of the rolling bearing has great significance.

The fault diagnosis of the rolling bearing based on the vibration signal is the most commonly used in practical applications. However, the rolling bearing vibration is a complex, non-stationary and dynamic process. The vibration signal can not be described with a fixed time or frequency function. This increases the difficulty of fault diagnosis [1]. It is the key of fault diagnosis to extract the fault feature from the vibration signal of the rolling bearing. The time-frequency analysis method has been widely used in the fault diagnosis of the rolling bearing because it provides the local information of vibration signal in the time and frequency domain [2, 3].

A lot of time-frequency analysis methods are used in the practical fault diagnosis, such as Wigner-Ville distribution, short-time Fourier transform (STFT) and empirical mode decomposition (EMD), etc. However, there are some limitations of these methods. Wigner-Ville distribution analysis of multi-component signal will occur cross terms [4]. As for the

STFT, the size of time-frequency window is fixed. The STFT divides the time-frequency plane used mechanical lattice. It is not an essentially adaptive signal processing method [5]. EMD is an adaptive signal processing method. It can adaptively divide complex multi-component signals into several IMF components. We can gain the integrated time-frequency distribution of the original signal by time-frequency analysis of the whole IMF components. However, in theory, there are some problems about EMD, such as over envelope, under envelope, modal confusion, and end effect, *etc.* [6]. The researchers proposed many methods in order to solve the above referred problems. Wu and Huang proposed EEMD decomposition method, based on depth studying the EMD decomposition of white-noise, and verified that EEMD has an effective anti-aliasing capability. However, it still not better solve the end effect. At the same time, the decomposed components may not meet an IMF [7], but we still regarded it as an IMF in practical application. Jonathan S. Smith proposed a decomposition method based on LMD on the basis of the previous studies. LMD is a new, adaptive and non-stationary signal processing method [8]. After LMD proposed, many scholars applied it to solve practical problems. Its application achieved very good results in the field of fault diagnosis [9, 10].

The vibration signal of rolling bearing fault is a multi-component signal combined frequency modulation (FM) with amplitude modulation (AM). Therefore, this paper proposed a fault diagnosis method of rolling bearing based on LMD and time-frequency analysis. Firstly, we need to gain the energy density distribution of signal using the time-frequency analysis of the PF which is decomposed by the LMD. Secondly, according to the energy density distribution, diagnose the yielded fault of rolling bearing. Finally, we compare simulation results using the proposed method with others, including the results achieved by using directly time-frequency analysis of signal and the time-frequency analysis of IMF decomposed by the EEMD of signal. We can verify the effectiveness of the proposed method.

$$xi(t) \square x(t) \square ni(t)$$

2. The Decomposition Principle of EEMD and

LMD 2.1. The decomposition principle of EEMD

The principle of EEMD method utilizes the statistical characteristics of Gaussian white-noise which has uniform distribution of frequency. The signal will have continuity on
358 different scales, to promote anti-aliasing decomposition and avoid modal confusion when

the white noise added into the original signal. Its specific decomposition steps and principle are as follows [11].

Step 1: Repeatedly add the white-noise into original signal. The mean value of white noise is 0; amplitude standard differential is constant. The standard differential of the white noise range is from 10 percent to 40 percent of original signal. The formula (1) is its mathematical expression.

$$x_i(t) = x(t) + n_i(t)$$

(1)

Here, it is the i th time that signal $x(t)$ has been added the white-noise. The size of the Gaussian white-noise will directly affect decomposition effect of avoiding modal confusion of the EEMD.

Step 2: Gain the IMF component denoted as $c_{j,i}(t)$ and remainder term denoted as $r_{j,i}(t)$ utilized the EEMD decomposition of $x_i(t)$. The $c_{j,i}(t)$ represents the j th IMF which gained by EMD decomposition of the $x_i(t)$.

Step 3: The step 1 and step 2 iterate N times. We make use of the principle of what the statistical mean of the unrelated random sequence is 0 to perform ensemble mean operator and eliminate the Gaussian white noise impact on the real IMF. The formula (2) is mathematical expression of the IMF of EEMD decomposition.

$$m_j^i = \frac{1}{N} \sum_{n=1}^N x_n^i \quad (2)$$

Here, the m_j^i represents the jth IMF which gained by EEMD decomposition of original signal. The sum of IMF which gained by EEMD decomposition of the white-noise will tend to 0 when N is very big. Now, the formula (3) is EEMD decomposition result.

$$m^i = \sum_{j=1}^J m_j^i + r^i \quad (3)$$

Here, r^i is the final remainder term. It represents the average trend of the signal. Any one signal can be decomposed into several IMFs and remainder term through the EEMD method. m_j^i (j=1, 2 ...) represents signal component of different frequency band which range from high to low. The frequency of every frequency band is different. It varies with the vibration of signal.

2.2. The decomposition principle of LMD

The substance of LMD method is separated the original signal to gain the pure FM signal and the envelope signal. The pure FM signal and envelope signal multiplication can get a PF, which is instantaneous frequency with the actual physical meaning. We can obtain all PFs from the original signal through the iterative processing. For any signal, the LMD decomposition processes are as follows [8].

- 1) Find out all local extremum points of the original signal and calculate the average of all adjacent local extremum points. The expression is as follows.

$$\bar{h}$$

$$\bar{c}_i = \frac{c_{i-1} + c_i + c_{i+1}}{3}$$

All adjacent average point \bar{c}_i is connected with a line and smoothed with a sliding average method to obtain a local mean function \bar{c}_i .

2) Calculate envelope estimation value. The formula (5) is the calculated mode.

(5)

All adjacent envelopes estimated value is connected with a line and smoothed with a sliding average method to get an envelope estimation function \bar{c}_i .

3) Separate local mean function from the original signal .we can achieve the formula (6) as follows.

$$(6)$$

4) Divide by envelope estimation function to achieve demodulation of the . We can achieve the formula (7).

$$(7)$$

For , iteration of the above steps can get the envelope estimation function of the signal . If is not equal to 1. It shows that is not a pure FM signal. Therefore, we can terminate iteration until is a pure FM signal. The number of iteration is n. The envelope estimation function of is . Therefore, this process is represented by the formula (8).

$$\begin{aligned}
 & \frac{f_{i1}}{f_{i1}} \\
 & \frac{x(t)}{m_{i1}(t)} \\
 & \dots \\
 & \dots
 \end{aligned}
 \tag{8}$$

In the formula (8),

$$\begin{aligned}
 & f_{i1}(\cdot) = f_{i1}(\cdot) / f_{i1}(\cdot) \\
 & \dots \\
 & \dots
 \end{aligned}$$

The termination condition of iteration is formula (10).

$$\begin{aligned}
 & \dots \\
 & \dots
 \end{aligned}
 \tag{10}$$

In the practical application, we can set a variable . Iteration can terminate when meets condition .

5) All envelopes generated by iterative process are multiplied by the estimated function to obtain an envelope signal (instantaneous amplitude function). The formula (11) describe this process.

$$p_1(t) \approx a_1(t) \cos(\omega_c t + \phi(t))$$

(11)

6) Envelope signal is multiplied by pure FM signal to obtain the first PF component of original signal. It can be represented by formula (12).

(12)

Here, $x(t)$ contains the highest frequency component of the original signal, and is an AM-FM signal of single component; the instantaneous amplitude is the envelope signal $A(t)$, the instantaneous frequency $f(t)$ can be obtained from the pure FM signal $\phi(t)$. The formula (13) is calculated mode of the $x(t)$.

$$x(t) = A(t) \cos(\phi(t)) \quad (13)$$

7) To obtain new signal $x_1(t)$, separate the first PF component $A_1(t)$ from the original signal $x(t)$. We regard $x_1(t)$ as the original signal and repeat the above steps until $x_n(t)$ is a monotonic function. The formula (14) is the iteration process.

$$x(t) = \sum_{i=1}^n A_i(t) \cos(\phi_i(t)) + r(t) \quad (14)$$

$\frac{u}{t}$
=



The original signal $x(t)$ can be reconstructed by all PFs component and $r(t)$. Formula (15) can represent this process.

$$x(t) = \sum_{i=1}^n A_i(t) \cos(\phi_i(t)) + r(t) \quad (15)$$

3. Time-frequency Analysis

The signal representation utilizing joint function of time and frequency referred to as time-frequency representation of signals, divided into both linear and quadratic time-frequency representation.

However, there are STFT and wavelet transform about the typical linear time-frequency representation. In many practical situations, the quadratic time-frequency representation will be described the distribution of the energy density of the signal, called the signal time-frequency distribution [12, 13].

In time-frequency analysis, we will mainly adopt the typical Wigner Ville distribution, STFT, the pseudo Margenau-Hill and Choi-Williams distribution to complete the subsequent time-frequency analysis of signal. The following is a brief description about using the time-frequency analysis method

3.1. Short-time Fourier Transform

In 1946, Dennis Gabor introduced the STFT. The basic idea is to use window function to intercept signal. It is assumed that the signal is stationary in the window. We analyze the intercept signal used the Fourier transform in order to determine the frequency components in the window. Then, we moved the window function along the time axis direction of signal to

obtain the variation of frequency with time. It is called time-frequency distribution [14, 15].

The STFT of the signal is represented by the formula (16).

$$(16)$$

In the formula (16), is original signal; $g(t)$ is window function. Its inverse transform is represented by the formula (17).

$$(17)$$

According to the formula (16) and (17), it is seen that the STFT calculate the frequency spectrum by sliding window. So its time and frequency resolution is constrained by Heisenberg's uncertainty principle. In other word, using short window higher time resolution can be gained, but frequency resolution is poor; using long window can gain higher frequency resolution, but time resolution is weak.

3.2. Cohen time-frequency distribution

Cohen [16] gave the general expression of time-frequency distribution for a given signal. The general form can be represented by the formula (18).

$$\int_{-\infty}^{\infty} \int_{-\infty}^{\infty} \dots$$

$$\cos(\omega t - \nu)$$

(1 8)

In the formula (18), $K(\omega, t)$ is Kernel function. If kernel function is given, the time-frequency distribution of signal $x(t)$ can be easily produced. Because the different of the time-frequency distribution is just reflected on the choice of kernel function form. Therefore, the formula (18) provides a general expression of any kind of time-frequency distribution.

The kernel function $K(\omega, t)$ can be related with signal $x(t)$. The signal becomes separable common form when kernel function is independent on the signal $x(t)$. The distribution is called bilinear structure of signal $x(t)$. Then the distribution characteristics are reflected on the kernel function $K(\omega, t)$.

If $K(\omega, t) = e^{j(\omega t - \nu)}$, the formula (18) becomes Winger-Wille distribution. The formula (19) is the mathematical expression of Winger-Wille distribution.

$$P_{MFT}(\omega, t) = \int_{-\infty}^{\infty} x(u) x^*(u + \tau) e^{j(\omega \tau - \nu)} du$$

$$\square \quad \quad \quad 2 \quad \quad 2 \quad \quad \quad (19)$$

$$\square \square \square \quad \quad \quad j2 \square (\square \square f_{uv}) \quad \quad *$$

If \square , the formula (18) becomes Margenau-Hill distribution. The formula (20) is the mathematical expression of Margenau-Hill distribution.

$$(20)$$

The cross terms is an inevitable trend of the bilinear time-frequency distribution. They come from the interactions of signal components of multi-component signal. We can see that

$$P = \frac{1}{\sqrt{2\pi}} \exp\left(-\frac{f^2}{2}\right)$$

Margenau-Hill distribution did not add any window function in the formula (20). If add the window function into the variable , we can reduce the cross terms. In this case, the distribution is called pseudo Margenau-Hill distribution. It can be expressed by the formula (21).

$$P = \frac{1}{\sqrt{2\pi}} \exp\left(-\frac{f^2}{2}\right) \exp\left(-\frac{a}{2}\right) \quad (21)$$

$$P(f, t) = \frac{1}{\sqrt{2\pi}} \exp\left(-\frac{f^2}{2}\right) \exp\left(-\frac{a}{2}\right) \exp\left(-\frac{r}{2}\right) \exp\left(-\frac{r}{2}\right) \quad (21)$$

If , the formula (18) becomes Choi-Williams distribution. The formula (22) is the mathematical expression of Choi-Williams distribution.

In the formula (22), is the attenuation coefficient, and it is proportional to the amplitude of the cross terms. The formula (22) is equivalent to the Wigner-Ville distribution when approaches infinity.

4. Experimental Simulation Demonstration

The experimental analysis data is Case Western Reserve University's experiment data of the rolling bearing in USA. It can be verified the effectiveness of the extraction feature and we propose method [17]. The detailed experimental parameters are as follows. The rolling bearing model is 6205-2RSJEMSKF; the vibration data was collected by using accelerometers, which were attached to the housing with magnetic bases and placed at the motor drive end; the motor speed is 1797rpm; the sampling frequency is 12KHZ; the sampling points selected data is 1000. The Normal, rolling element fault, inner ring fault and outer ring fault vibration signals of the rolling bearing were selected to conduct experimental simulation.

According to the theoretical formula which is presented in the literature [18] based on the above parameters setting, we can calculate the fault characteristic frequency. The fault characteristic frequency is shown in Table 1.

Next, we compare diagnosis effect achieved by using directly time-frequency analysis of signal with the time-frequency analysis of IMF which is decomposed by EEMD of signal, and the time-frequency analysis of PF decomposed by LMD. The energy density distribution of the signal is obtained by time-frequency analysis. We can diagnose the rolling bearing

fault used the energy density distribution of the signal. The simulation results show that we can gain the clearer the energy density distribution by the time-frequency of PF of signal.

Especially in Wigner Ville distribution and pseudo Margenau-Hill distribution analysis, the effect is more obvious.

Table 1. Fault characteristic frequency (unit: HZ)

<u>outer ring fault</u>	<u>inner ring fault</u>	<u>rolling element fault</u>
107.3648	162.1852	141.1693



4.1. The vibration signal analysis of the normal rolling bearing

The vibration signal of simulation outer ring fault of rolling bearing is conducted the subsequent analysis. The type of simulation outer ring fault is single little corrosion fault and the fault diameter is 0.007 inches. The simulation results are shown in Figure 1 to Figure 5.

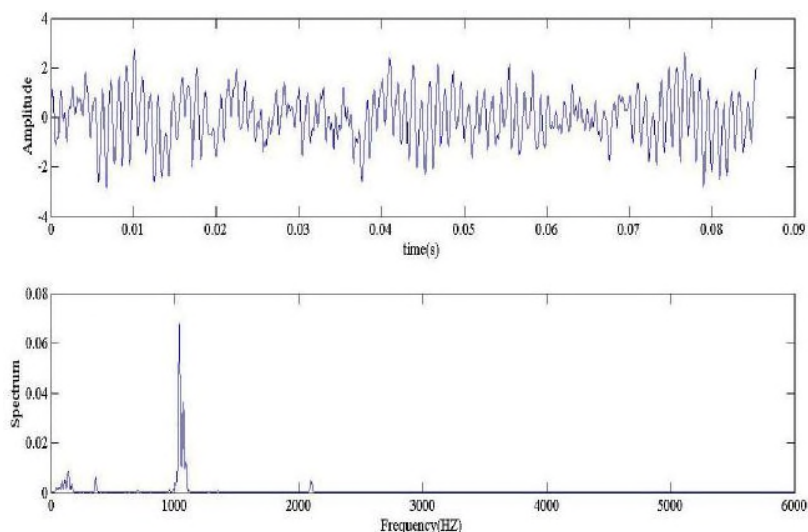


Figure 1. The time domain and power spectrum waveform of the normal rolling bearing signal

The simulation results of the inner ring fault of rolling bearing signal are shown in the Figure 1 to Figure 5. In the Figure 1, as it is been seen, the vibration signal of the rolling bearing is not obvious impact spike and the amplitude change is relatively stable. In the Figure 2, Figure 3 and Figure 5, the simulation results show that the energy density distribution of the vibration signal of the normal rolling bearing is mainly concentrated in the 1000HZ nearby.

We compare simulation results achieved by directly time-frequency analysis of signal and the time-frequency analysis of IMF which is decomposed by the EEMD of signal and the time-frequency analysis of PF decomposed by the LMD. At the same time, we can also conclude that the analysis effect used the STFT is poorer in all utilized time-frequency methods. It is related with the limitations of STFT and it belongs to linear time-frequency representation.

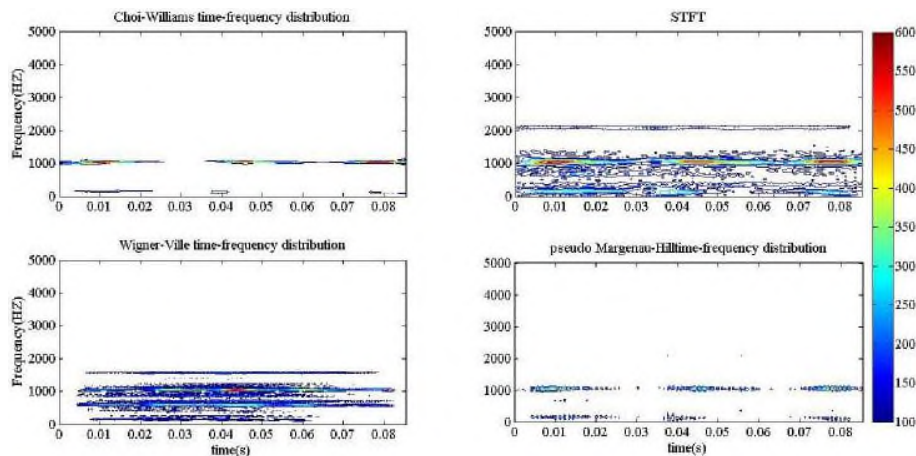


Figure 2. The direct time-frequency analysis of the normal rolling bearing signal

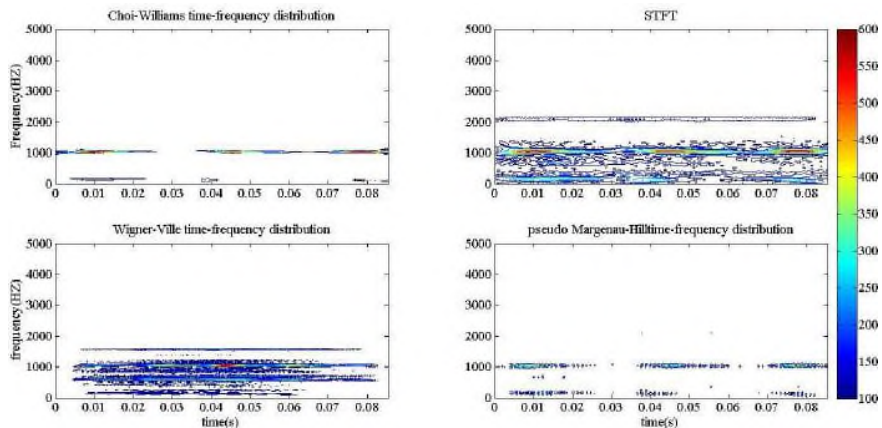


Figure 3. The time-frequency analysis of IMF decomposed by EEMD of the normal rolling bearing signal

4.2. The vibration signal analysis of the inner ring fault

The vibration signal of simulation inner ring fault of rolling bearing is analyzed to further verify the effectiveness of the proposed method. The type of simulation inner ring fault is single little corrosion fault and the fault diameter is 0.007 inches. The simulation results are shown in Figure 6 to Figure 10.

The simulation results of the inner ring fault of rolling bearing signal are shown in the Figure 6 to Figure 10. In the Figure 6, as it is been seen, the vibration signal of the inner ring fault increases obviously impact spike. There are many frequency components with large amplitude in the power spectrum. But we can't directly extract the feature frequency of inner ring fault from the time domain and power spectrum to diagnose the fault. Therefore, we design a digital low-pass filter whose cut-off frequency is 500HZ [19] based on the calculated fault characteristic frequency in the Table 1.

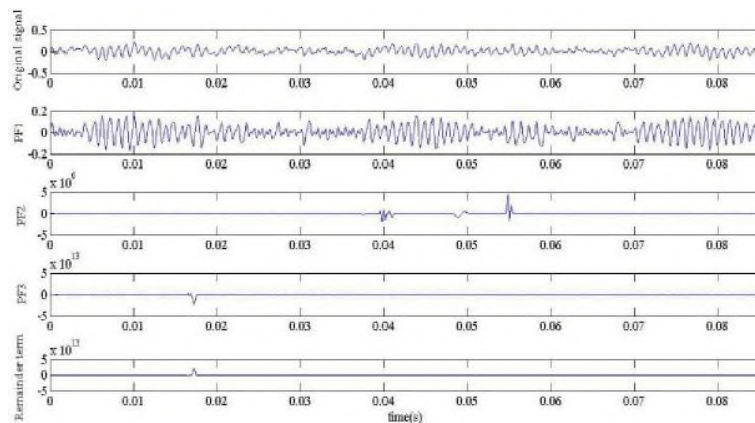


Figure 4. The LMD decomposition diagram of the normal rolling bearing signal

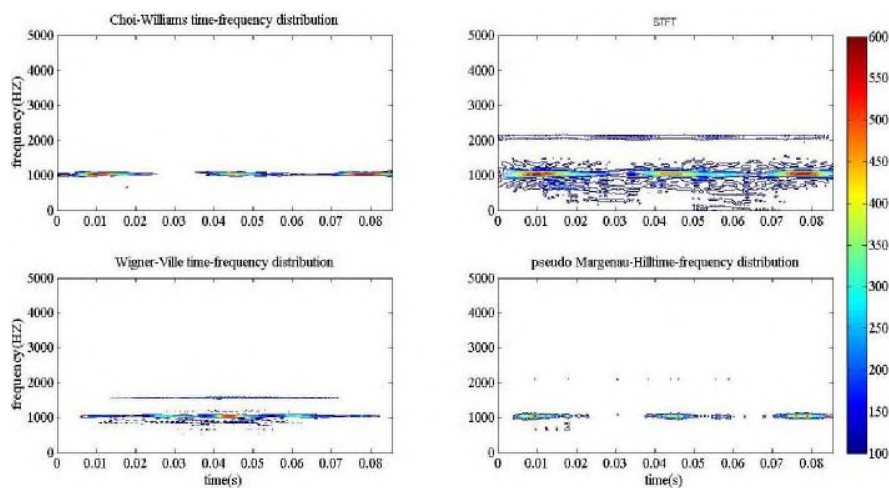


Figure 5. The time-frequency analysis of PF decomposed by LMD of the normal rolling bearing signal

Next, we conduct filter to the signal used the designed filter, and perform the subsequent time-frequency analysis. In time-frequency analysis chart, the red baseline ($=162.1852\text{HZ}$) is the inner ring fault characteristic frequency.

In the Figure 7, Figure 8 and Figure 10, as it is been seen clearly, the energy density distribution is mainly concentrated in the inner ring fault characteristic frequency nearby. It shows that the inner ring of the rolling bearing has occurred fault. However, the above-mentioned three methods can judge whether the inner ring occur fault. We can't declare the superiority of the proposed method. Then the vibration signal of simulation rolling element and outer ring fault of rolling bearing are analyzed to further verify validity and superiority of the proposed method

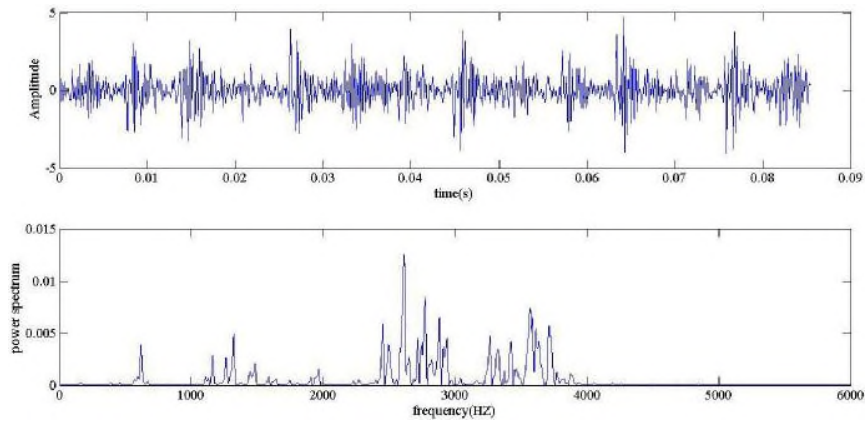


Figure 6. The time domain and power spectrum waveform of the inner ring fault

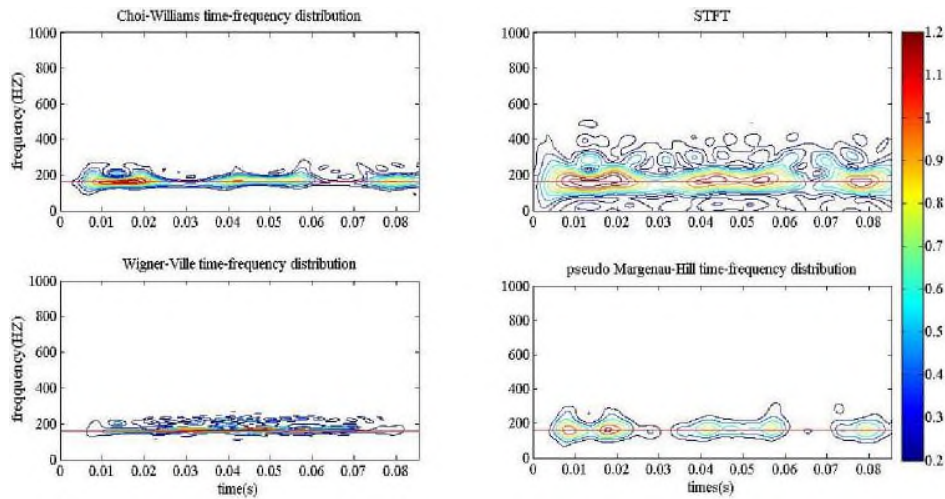


Figure 7. The direct time-frequency analysis of the inner ring fault

4.3. The vibration signal analysis of the rolling element fault

The analysis of the vibration signal of the rolling element is similar with the analysis of inner ring fault. The results are shown in the Figure 11 to Figure 15.

In the Figure 11, as it is been seen, the vibration signal of the rolling element fault increases obviously impact spike. There are many frequency components with large amplitude in the spectrum. But we can't directly extract the feature frequency of rolling element fault from the time domain and power spectrum to diagnose the fault. Therefore, according to the calculated fault characteristic frequency in the Table 1, we design a digital low-pass filter, whose cut-off frequency is 400HZ.

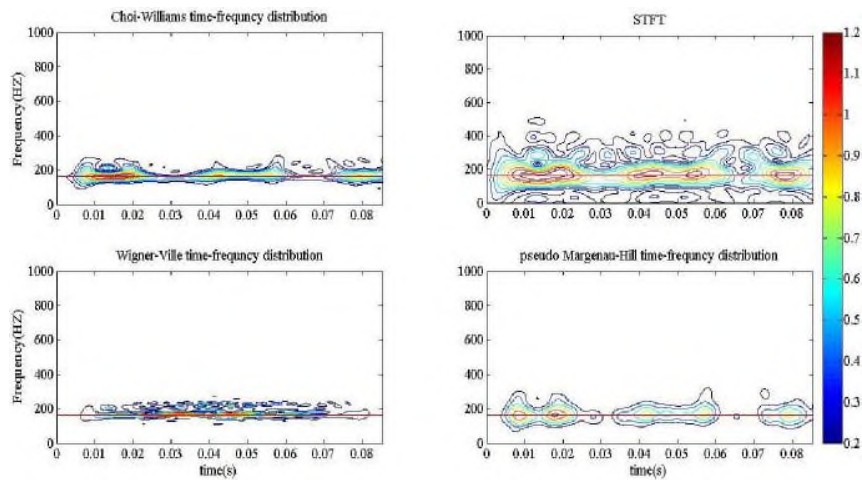


Figure 8. The time-frequency analysis of IMF decomposed by EMD of the inner ring fault

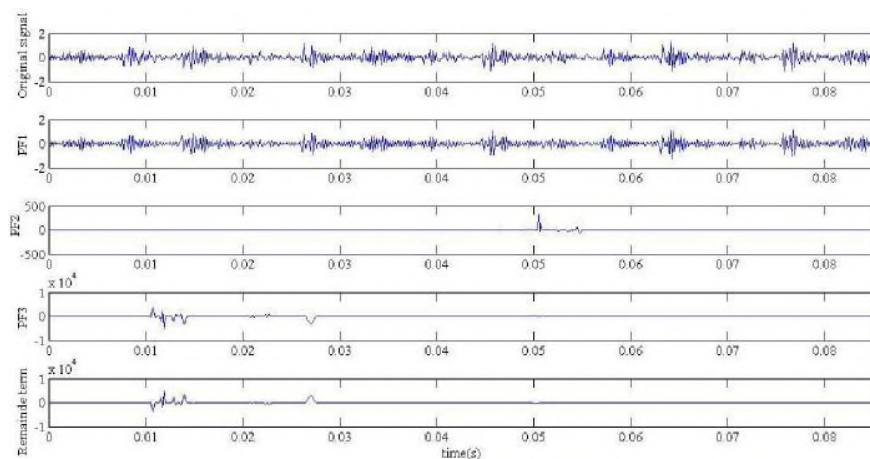


Figure 9. The LMD decomposition diagram of the inner ring fault

Next, we conduct filter to the signal used the designed filter, and perform the subsequent time-frequency analysis. In time-frequency analysis chart, the red baseline ($=141.1693\text{HZ}$) is the fault characteristic frequency of the rolling element of the rolling bearing.

In the Figure 12, Figure 13 and Figure 15, as it is been seen, the energy density distribution is mainly concentrated in the rolling element fault characteristic frequency nearby. It shows that the rolling element of the rolling bearing has occurred fault. However, the effect of the time-frequency analysis is different. The energy desity distribution of the time-frequency analysis of PF is more concentrated.

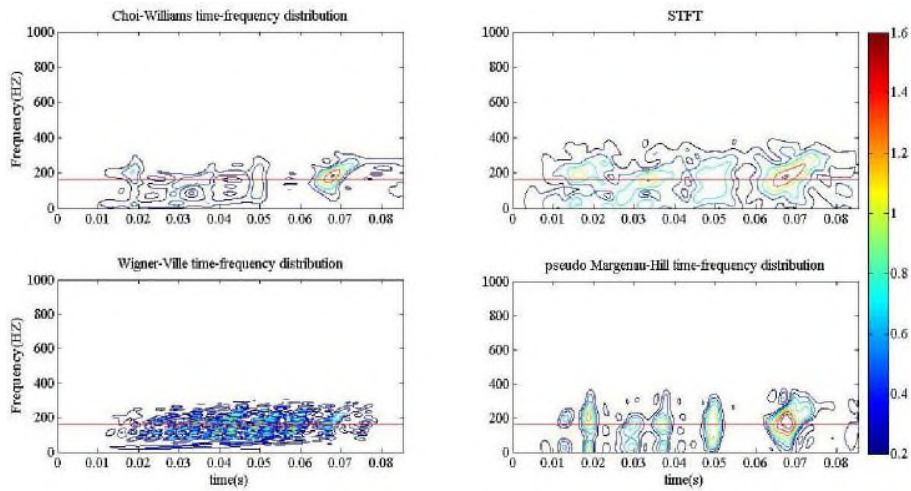


Figure 10. The time-frequency analysis of PF decomposed by LMD of the inner ring fault

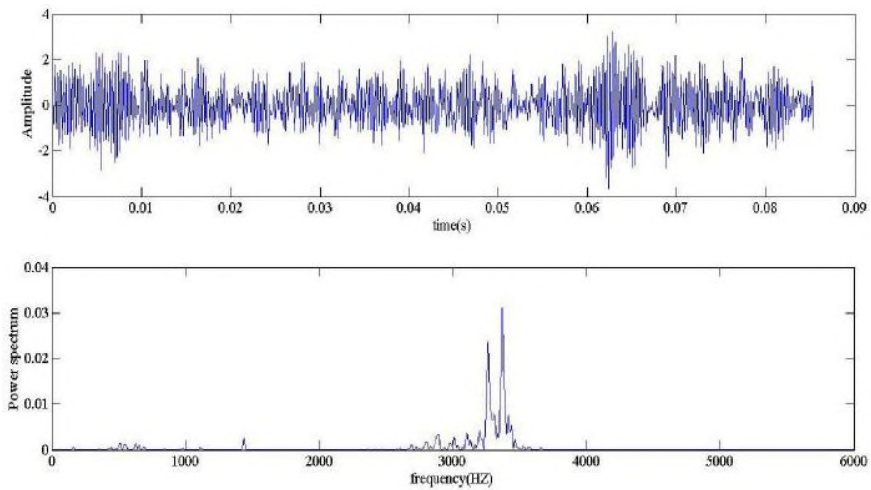


Figure 11. The time domain and power spectrum waveform of the rolling element fault

4.4. The vibration signal analysis of the outer ring fault

The vibration signal of simulation outer ring fault of rolling bearing is conducted the subsequent analysis. The type of simulation outer ring fault is single little corrosion fault and the fault diameter is 0.007 inches. The simulation results are shown in Figure 16 to Figure 20.

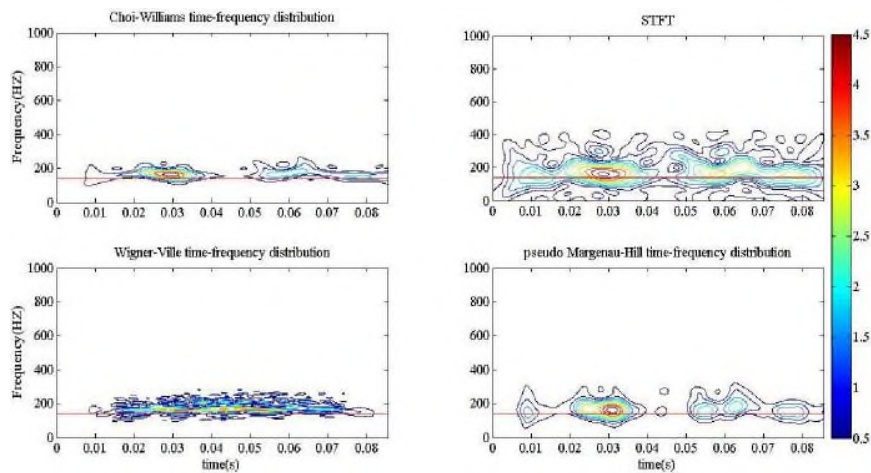


Figure 12. The direct time-frequency analysis of the rolling element fault

In the Figure 16, as it is been seen, the vibration signal of the outer ring fault is obvious impact spike. There are many frequency components with large amplitude in the spectrum. But we can't directly extract the feature frequency of outer ring fault from the time domain and power spectrum to diagnose the fault.

Therefore, we design a digital low-pass filter whose cut-off frequency is 300HZ based on the calculated fault characteristic frequency in the Table 1. Next, we conduct filter to the signal used the designed filter, and perform the subsequent time-frequency analysis to the filtered signal.

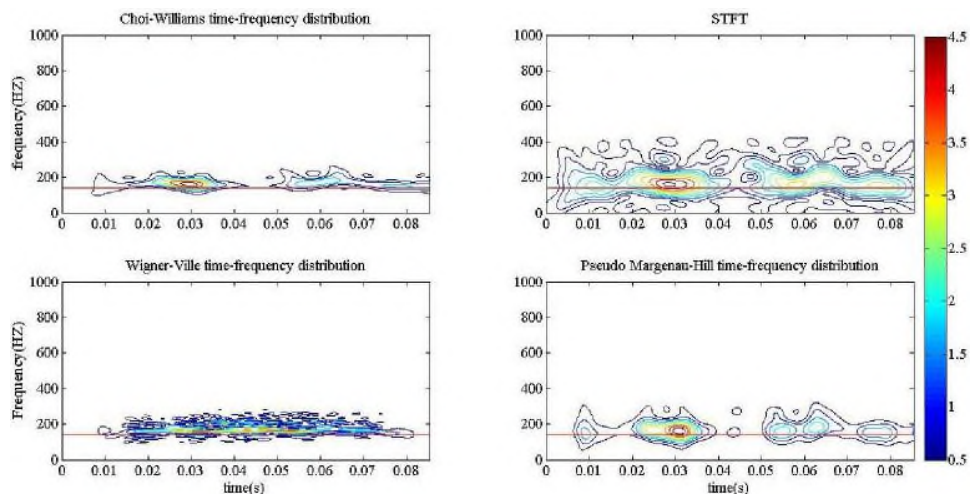


Figure 13. The time-frequency analysis of IMF decomposed by EEMD of the rolling element fault

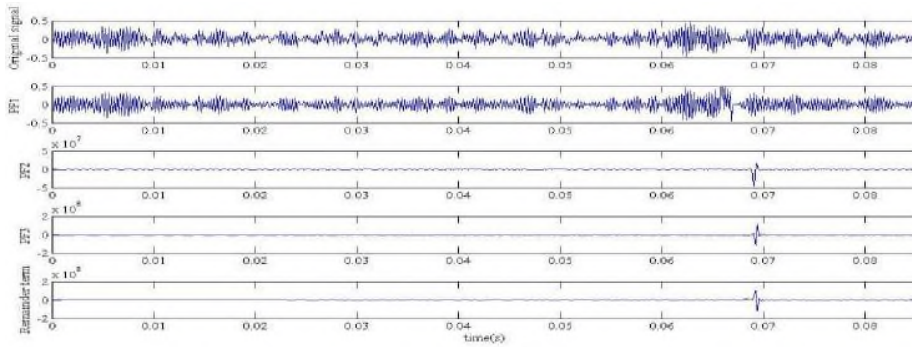


Figure 14. The LMD decomposition diagram of the rolling element fault

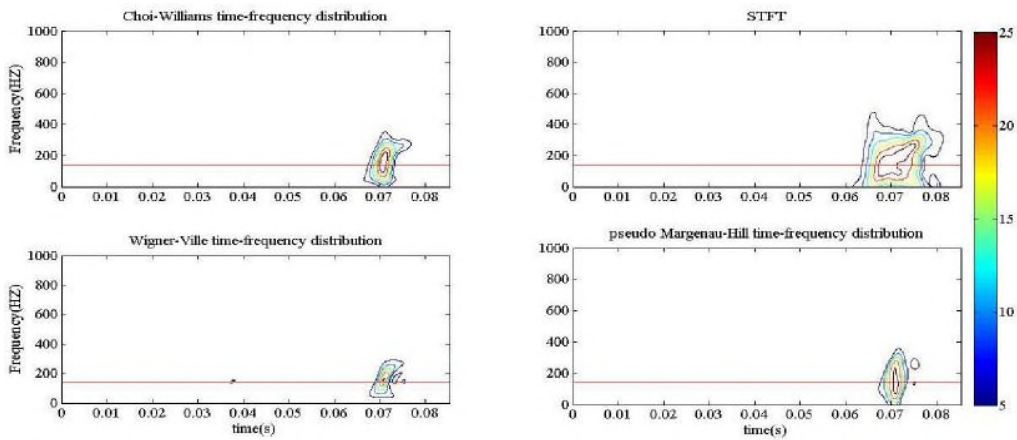


Figure 15. The time-frequency analysis of PF decomposed by LMD of the rolling element fault

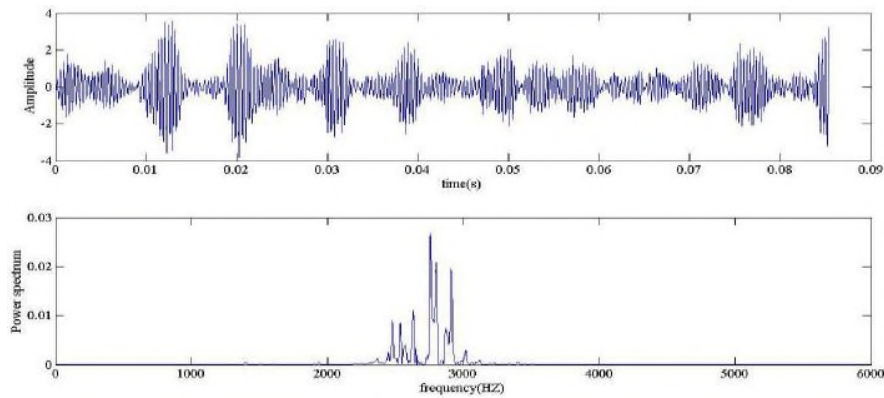


Figure 16. The time domain and power spectrum waveform of the outer ring fault

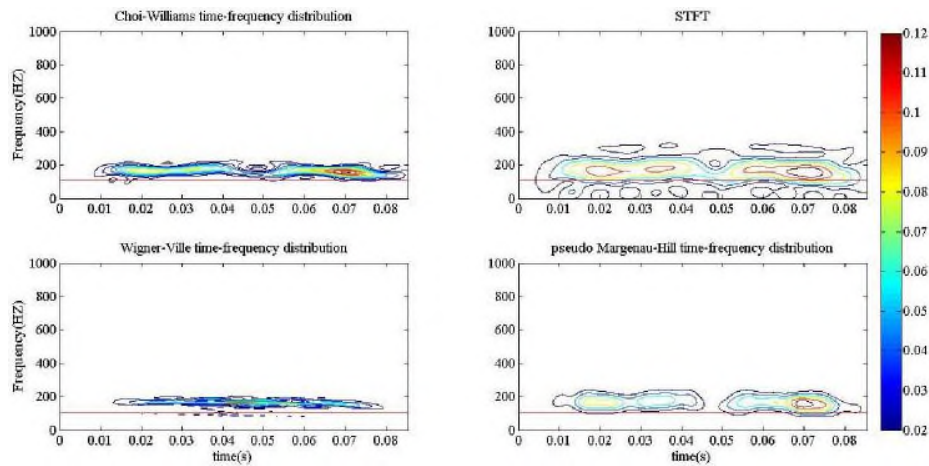


Figure 17. The direct time-frequency analysis of the outer ring fault

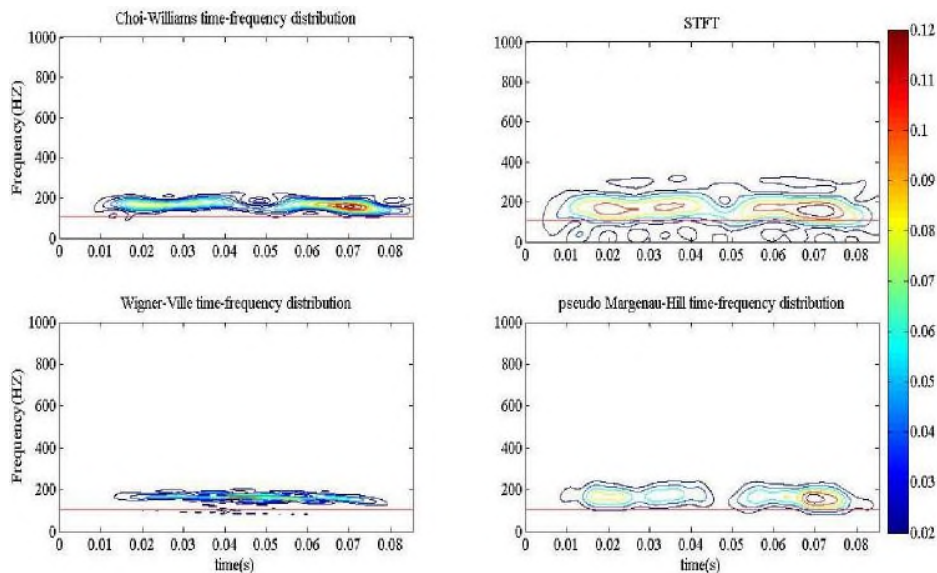


Figure 18. The ime-frequency analysis of IMF decomposed by EEMD of outer ring fault

In time-frequency analysis chart, the red baseline ($\omega = 107.348\text{HZ}$) is the fault characteristic frequency of the outer ring. In the Figure 20, as it is been seen, the energy density distribution is mainly concentrated in the fault characteristic frequency of the outer ring nearby. It shows that the outer ring of the rolling bearing has occurred fault. However, in the Figure 17 and Figure 18, the energy density distribution deviates seriously from the red baseline. We don't determine whether the outer ring has occur. The result adequately verifies the effectiveness of the proposed method.

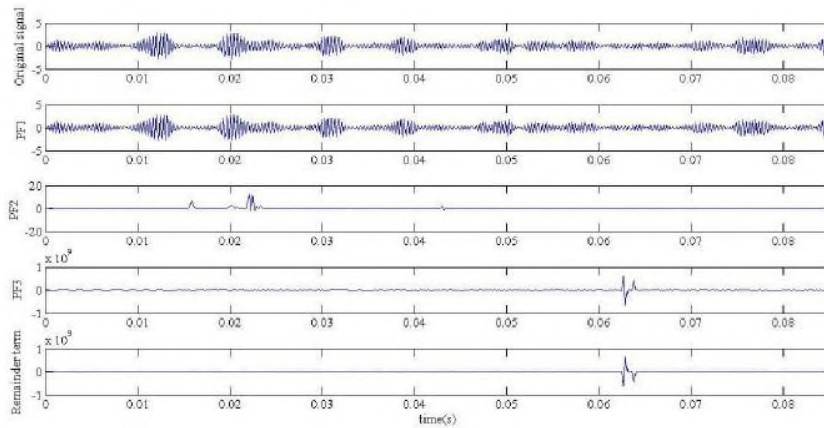


Figure 19. The LMD decomposition diagram of the outer ring fault

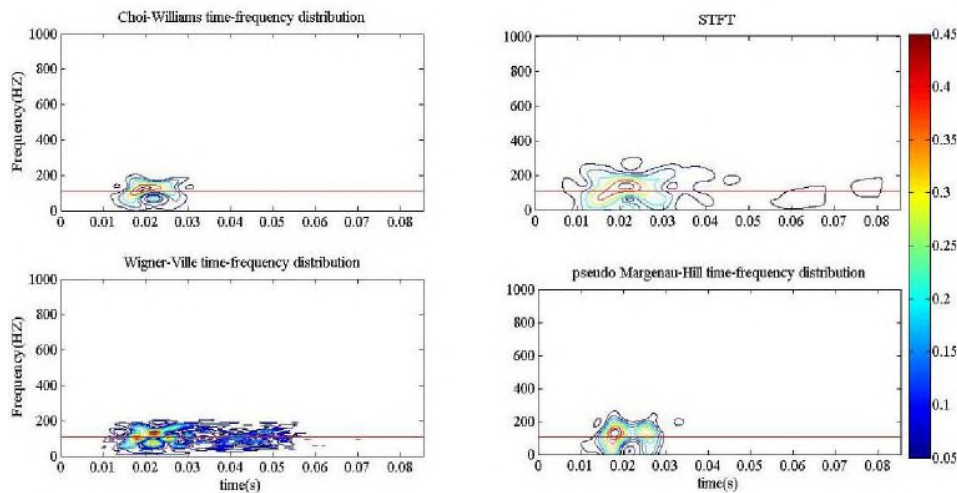


Figure 20. The time-frequency analysis of PF decomposed by LMD of the outer ring fault

5. Conclusions

The above analyzed results show that LMD is an adaptive analysis method based on the characteristics of the signal itself. We can gain the clearer energy density distribution which is gained by time-frequency analysis of every PF. The time-frequency energy density distribution determines the variation of the frequency with time. Therefore, it can be used to diagnose the yielded fault. The diagnosis result of the proposed method is better than results which are achieved by directly time-frequency analysis of signal and the time-frequency analysis of IMF decomposed by EEMD of signal. However, the end points of the LMD decomposition are processed by the symmetric extreme extension method and not proceeded the profound studying about the eliminating end effect.

So, we can expand the studying of LMD decomposition details, such as adaptive endpoint extension, the mechanism of end effect, *etc.*

Acknowledgements

*(Jiande Wu) is the corresponding author. This paper is supported by the foundation items: Project supported by Natural Science Foundation of China (Grant No. 51169007), Science & Research Program of Yunnan province (No. 2010DH004 & No.2011CI017 & No.2011DA005 & 2011FZ036 & 2012CA022), Foundation of Yunnan Education Department (2011Y386).

References

- [1] T. Peng Tao, H. Yang, J. Li, H. Jiang and W. Wei, "Mixed-domain feature extraction approach to rolling bearings faults based on kernel principle component analysis", *Journal of Central South University (Science and Technology)*, vol. 42, (2011), pp. 3384-3391.
- [2] N. G. Nikolaou and I. A. Antoniadis, "Rolling element bearing fault diagnosis using Wavelet Packets", *NDT & International*, vol. 35, (2002), pp. 179-205.
- [3] Z. K. Peng, P. W. Tse and F. L. Chu, "An Improved Hilbert-Huang Transform and Its Application in Vibration Signal Analysis", *Journal of Sound and Vibration*, vol. 286, (2005), pp. 187-205.
- [4] J. -H. Lee, J. Kim and H. -J. Kim, "Development of enhanced Wigner-Ville distribution Function", *Mechanical Systems and Signal Processing*, vol. 13, no. 2, (2001), pp. 367-398.
- [5] L. Cohen, "Time-frequency Distribution-A Review", *Proceedings of the IEEE*, vol. 77, no. 7, (1989), pp. 941-981.
- [6] N. E. Huang, Z. Shen, S. R. Long, M. C. Wu, H. H. Shih, Q. Zheng, N. -C. Yen, C. C. Tung and H. H. Liu, "The Empirical Mode Decomposition and the Hilbert Spectrum for Nonlinear and Non-stationary Time Series Analysis", *Proc. R. Soc. Lond. A*, vol. 454, no. 1971, (1998), pp. 903-995.
- [7] C. Zhang and J. Chen, "Contrast of Ensemble Empirical Mode Decomposition and Empirical Mode Decomposition in Modal Mixture", *Journal of Vibration and Shock*, no. 29, (2010).
- [8] J. S. Smith, "The Local Mean Decomposition and Its Application to EEG Perception Data", *Journal of the Royal Society Interface*, vol. 2, no. 5, (2005), pp. 443-454.
- [9] Y. Yang, J. Cheng and K. Zhang, "An ensemble local means decomposition method and its application to local rub-impact fault diagnosis of the rotor systems", *Measurement*, vol. 45, no. 3, (2012), pp. 561-570.
- [10] J. -s. Cheng, Y. Yang and Y. Yang, "A rotating machinery fault diagnosis method based on local mean decomposition", *Digital Signal Processing*, vol. 22, no. 2, (2012), pp. 356-366.
- [11] L. Chen, Y. Zi, Z. He and W. Cheng, "Research and Application of Ensemble Empirical Mode Decomposition Principle and 1.5 Dimension Spectrum Method", *Journal of Xi'an Jiaotong University*, vol. 43, no. 5, (2009), pp. 94-98.
- [12] Z. Ge and Z. Chen, "Matlab Time-Frequency Analysis and Its Applications", *Posts & Telecom Press*, vol. 1, (2006), pp. 2-17.
- [13] J. Treetrong, "Fault Detection of Electric Motors Based on Frequency and TimeFrequency Analysis using Extended DFT", http://www.sersc.org/journals/IJCA/vol4_no1/4.pdf.
- [14] M. Latfaoui and F. B. Reguig, "Time-Frequency Analysis of Femoral and Carotid Arterial Doppler Signals", *Procedia Engineering*, vol. 29, (2012), pp. 3434-3441.
- [15] A. Kumar, G. Saranya, R. Selvakumar, S. Shree and M. Saranya, "Fault detection in Induction motor using WPT and Multiple SVM", http://www.sersc.org/journals/IJCA/vol3_no2/2.pdf.
- [16] L. Rilong and F. Zhihua, "Application of Margenau-Hill Distribution to Fault Identification of Bearing", *Journal of Vibration and Shock*, vol. 25, no. 2, (2006), pp. 175-177.
- [17] K. A. Loparo, "Bearings vibration data set [EB/OL]", Case Western Reserve University, <http://www.eecs.cwru.edu/laboratory/bearing/download.htm>.
- [18] X. Gao, "The precision diagnosis technology of fault in the Rolling bearing", *Non-ferrous equipment*, no. 3, (1994), pp. 29-39.
- [19] J. Park, Y. Ha and W. Chung, "Kalman Filtering based Adaptive Frequency Domain Channel Estimation with Low Pilot Overhead for OFDM Systems", http://www.sersc.org/journals/IJCA/vol5_no2/13.pdf.

Authors



Jun Ma

Jun Ma, born in 1989, is a postgraduate of Kunming University of Science and Technology. His main research interests on fault diagnosis and pattern recognition.



Jiande Wu

Jiande Wu is a professor of faculty of information engineering and automation, Kunming University of Science and Technology. He got the Master degree from northwestern polytechnical university, china in 2004, and PhD degree from Control science and Engineering Department, Zhejiang University in 2007. He has published more than 50 papers on international journals, national journals, and conferences in recent years. His research interests include: detection and control of pipe transportation technology.



Xuyi Yuan

Xuyi Yuan, born in 1987, is a postgraduate of Kunming University of Science and Technology. His main research interests on measuring technology and instruments.

